Journal of the European Ceramic Society 22 (2002) 883–890

www.elsevier.com/locate/jeurceramsoc

Effect of iron oxide content on the crystallisation of a diopside glass–ceramic glaze

M. Romero[a,*], J. Ma. Rincón[a], A. Acosta[b]

[a]*Instituto Eduardo Torroja de Ciencias de la Construcción, Laboratory of Glass–ceramic Materials, CSIC, Serrano Galvache s/n, 28033, Madrid, Spain*

[b]*Universidad de Castilla-La Mancha, Facultad de CC. Quimicas, Dpto. Mineralogia Aplicada, Avda. Camilo José Cela 10, 13071, Ciudad Real, Spain*

Received 16 February 2001; received in revised form 25 June 2001; accepted 9 July 2001

Abstract

The effect of iron oxide content on the crystallisation of a diopside glass–ceramic glaze was investigated using a glass–ceramic frit in the K_2O–ZnO–MgO–CaO–Al_2O_3–SiO_2 system and a granite waste glass. Measurements by X-ray diffraction (XRD) combined with scanning electron microscopy (SEM) and EDX microanalysis showed that the distribution of Fe^{3+} ions among different crystalline phases such as franklinite ($ZnFe_2O_4$) and hematite Fe_2O_3 depends on the iron content in the original diopside mixture. Thus, the original glaze crystallises to franklinite or hematatite when iron content is greater than 2 and 15%, respectively.

Keywords: Crystallization; Diopside frit; Fe_2O_3; Glass ceramics; Waste materials; $ZnFe_2O_4$

1. Introduction

The "frit" term points out a glassy mixture melted and sharply quenched in cool water, which is the basis of glazes and enamels used as coatings over ceramic and metallic substrates. There are a wide variety of frits, which have different features such as fusibility, gloss and opacity. Among the wide range of commercial frits, the so-called crystalline frits are of great interest. Crystalline frits, which are glossy, transparent, viscous and with low fusibility, are composed by SiO_2 (50–60 wt.%) and fluxing oxides such as Na_2O, K_2O, PbO and B_2O_3 (20–25 wt.%) as major components and stabilizing elements such as ZnO, Al_2O_3, CaO, BaO, MgO as minor components (7–9 wt.% maximum). As its name indicates, this type of frit is not totally glassy, showing certain grade of crystallisation. Diopside frits, which gives rise to high erosion and corrosion resistant tiles, are one of the most commonly commercialised crystalline frits.[1]

Glass and glass–ceramics frits have traditionally been made from pure raw materials. The scarcity of many of these has caused a necessity for the use of complementary raw materials. Moreover, a major problem in developed countries is the large quantity of inorganic solid wastes that are generated and which have to be disposed of. Hence, the use of these residues as secondary raw material in glass and glass–ceramic production seem to be the most promising way for its reuse. Thus, several works have been published regarding the fabrication of bulk glass–ceramics from different inorganic wastes, such as red muds from zinc hydrometallurgy,[2,3] coal fly ash,[4,5] iron blast-furnace slags[6] and filter dust from waste incinerators.[7–11] However, limited work has been published regarding the fabrication of glass–ceramics glazes from wastes. These few works include glass–ceramics glazes from metallurgical slags.[12] To our knowledge, however, granite wastes have not yet been considered in this regard.

Granite wastes are iron enriched residues composed by SiO_2, Al_2O_3 and Fe_2O_3 as major elements. The way in which iron is incorporated into bulk silicate glasses and the behaviour of iron-containing oxide glasses with heat-treatment to produce glass–ceramics have been a subject of considerable interest specially in determining the magnetic properties of the resultant materials[13] Work dealing with solid solution formation, phase relation and crystallisation characteristics of bulk glasses

* Corresponding author.
E-mail address: mromero@ietcc.csic.es (M. Romero).

0955-2219/02/$ - see front matter
PII: S0955-2219(01)00395-8

in the CaO–MgO–Fe_2O_3–SiO_2 basis system, including diopside and iron containing pyroxenes, has been reported in the literature.[14] However, to our knowledge, no previous work has been published regarding the effect of Fe_2O_3 on the crystallisation of a diopside glass–ceramic glaze. The present work was undertaken to determine how the crystallisation and the distribution of iron ions among different crystalline phases in a diopside glaze is affected by iron content.

2. Materials and methods

Diopside glassy frit was supplied by Fritta S.L. (Castellón, Spain). An iron rich waste originated by a Spanish granite plant was used to prepare an iron glass. The granite waste, which was supplied as a dried mud coming from the sawing processing of granite blocks, was melted in air at 1450 °C for 1 h in silica-alumina crucibles. The fluid melt was quenched by pouring into water to obtain a glassy frit. No visible corrosion or chemical attack of the silica-alumina crucible by the melt was observed. Chemical compositions of frits were measured by wet chemistry using inductively coupled plasma emission spectroscopy (ICP).

Both diopside and granite frits were crushed and sieved to <65 μm particle size. Different frits mixtures were prepared from diopside and granite frits as explained afterwards.

All frits mixtures were mixed with water and organic additives (TPF and DMC) in order to obtain a slip, which was poured onto 80×80 mm^2 fired ceramic tiles to produce a coating with a thickness of ≈ 500 μm. The coated tiles were dried in air for 24 h and heat treated at 1120 °C for 15 min with heating and cooling rates of 50 °C/min.

The glassy nature of diopside and granite frits as well as the evolution of crystalline phases developed in glaze tiles after heat treatment were determined by X-ray diffraction in a Philiphs X'PERT MPD diffractometer with CuK_α radiation. Scanning electron microscopy (SEM) on the surface of both as-produced and etched samples (2% HF for 1 min) was used to examine the microstructure of the glass–ceramic glazes. SEM observation were carried out in a Philips microscope at an acceleration voltage of 20 kV and energy dispersive X-ray (EDX) analysis with a solid state detector (Be window).

3. Results and discussion

Table 1 shows the chemical analysis by ICP of diopside and granite frits. In this Table, Fe_2O_3 represents the total amount of $FeO+Fe_2O_3$ in the granite frit. As expected, the major components in diopside frit are SiO_2, CaO, Al_2O_3 and ZnO, whereas granite frit is mainly composed by SiO_2, Fe_2O_3 and Al_2O_3.

Table 2 collects the different mixtures prepared from diopside and granite frits. The iron content of those mixtures is also showed in Table 2. As noted, the Fe_2O_3 content ranges from 0 wt.% in 100D mixture, which is only composed by diopside frit, to near 16% for 10D mixture, which is prepared with addition of a 90% of granite frit.

The frit mixtures were applied over ceramic tiles substrates as explained earlier. After cooling at room temperature, glaze tiles showed homogeneous and glossy surface. Glaze defects as bubbles or crazing were not detectable.

Fig. 1 shows the X-ray spectra collected on the surface of glaze tiles. The XRD pattern of sample 100D (Fig. 1a), which is prepared without addition of granite frit, shows that diopside frit gives rise to a glass–ceramic glaze comprised by diopside ($CaMg(SiO_3)_2$) and petedunnite ($CaZn(SiO_3)_2$). The DRX pattern of these two crystalline phases are very similar with diffractions peaks appearing at the same d value. For this reason, both phases are overlapped in the DRX diffractogram recorded on the surface of sample 100D. The microstructure of 100D glaze is presented in Fig. 2. The surface of the glaze is fully crystallised (Fig. 2a) and the microstructure is composed of parallelepiped and sail-like crystals (Fig. 2b). Parallelepiped crystals (Fig. 2c) shows an average size of 2×1.5 μm whereas the length of sail-like crystals is in the 3–5 μm range (Fig. 2d). Table 3

Table 1
Chemical composition (by ICP methods) of diopside and granite frits

	Diopside frit	Granite frit
SiO_2	60.80	55.24
Al_2O_3	6.60	12.42
Fe_2O_3	–	17.79
CaO	13.63	5.89
MgO	1.65	1.83
MnO	–	0.16
BaO	0.01	0.06
ZnO	11.71	0.11
Na_2O	0.90	2.64
K_2O	4.58	3.34
TiO_2	0.04	0.35
P_2O_5	–	0.16

Table 2
Original frits mixtures prepared from diopside and granite frits

Frit mixture	Diopside frit (wt.%)	Granite frit (wt.%)	Fe_2O_3 content (wt.%)
100D	100	0	0.00
90D	90	10	1.78
70D	70	30	5.34
50D	50	50	8.89
30D	30	70	12.45
10D	10	90	16.01

gives the chemical composition of 100D glaze and of the different phases as analysed by EDX. There are no significant differences between the compositions of glassy phase surrounding the two type of crystals. Thus, both crystalline phase grow from the same parent glass. The SiO_2 content is similar in the residual glass and in the crystalline phases being the Al_2O_3, CaO, MgO and K_2O contents the major difference between glassy and crystalline

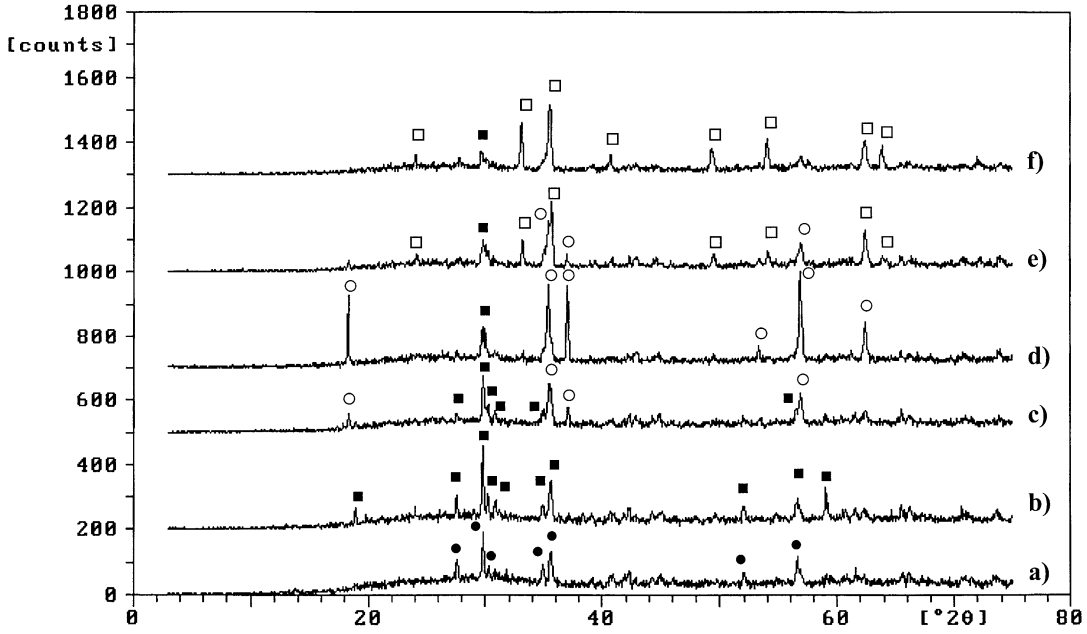

Fig. 1. X-ray spectra collected on the surface of glaze tiles: (a) 100D glaze; (b) 90D glaze; (c) 70D glaze; (d) 50D glaze; (e) 30D glaze and (f) 10D glaze (● = diopside ($CaMg(SiO_3)_2$) + petedunnite ($CaZn(SiO_3)_2$); ■ = diopside + petedunnite + augite ($Ca(Mg, Fe)(SiO_3)_2$); ○ = franklinite ($ZnFe_2O_4$); □ = hematite (Fe_2O_3)).

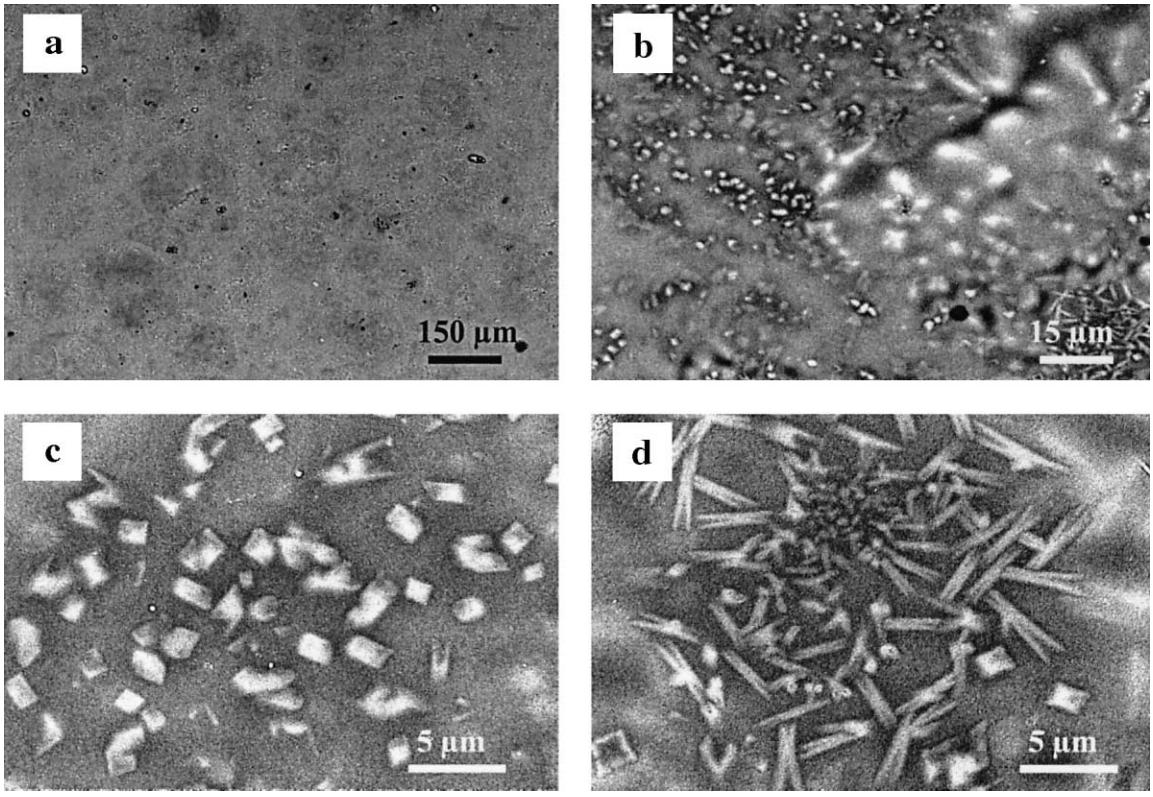

Fig. 2. SEM observations on the surface of 100D glass–ceramic glaze.

phase. The residual glassy phase is enriched in Al_2O_3 and K_2O while the CaO content is greater inside the crystals. As for MgO, its relative content between crystalline and glassy phase is dependent on the type of crystals. Thus, MgO content increases in the residual glassy phase when crystallisation of sail-like crystals takes place and decreases when parallelepiped crystals grow from the parent glass. Concerning to crystalline phases, the main difference between parallelepiped and sail-like crystals is the MgO and ZnO contents. MgO is not present in sail-like crystals, which show greater ZnO content. EDX and XRD results indicate that parallelepiped crystals correspond to diopside, whereas sail-like crystals correspond to petedunnite phase.

Fig. 3 shows the microstructure of 90D glaze prepared with addition of a 10% of granite frit. As well as 100D sample, the surface of 90D glaze is fully crystallised but new crystalline regions with high white contrast appears

Table 3
Chemical composition of 100D glaze and of the different phases as analysed by EDX spectrometry

	SiO_2	Al_2O_3	CaO	MgO	ZnO	K_2O
Average	66.46	8.47	12.51	1.16	8.46	2.94
Parallelepiped crystals	62.35	6.58	13.24	6.67	8.86	1.49
Sail-like crystals	63.42	7.23	13.69	0.00	12.63	2.06
Glassy phase surrounding parallelepiped crystals	63.98	8.37	11.88	2.04	10.64	3.10
Glassy phase surrounding sail-like crystals	62.67	8.78	12.18	1.57	11.99	2.81

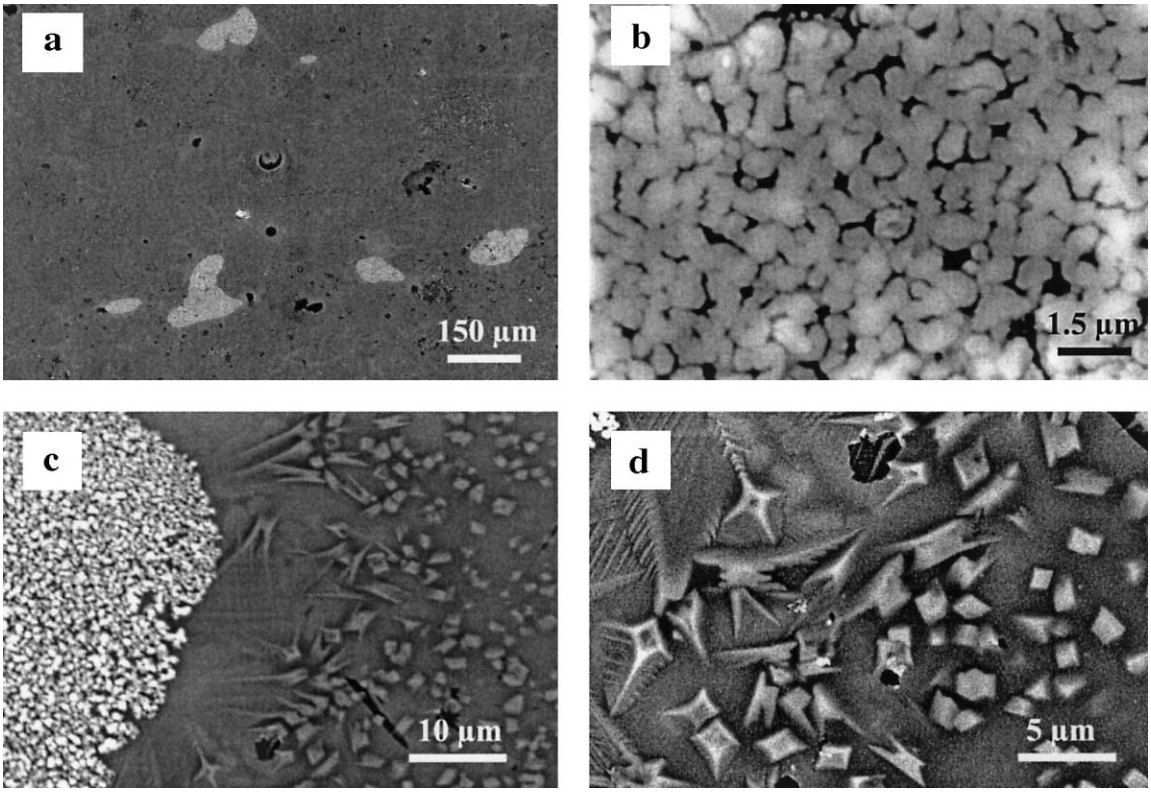

Fig. 3. SEM observations on the surface of 90D glass–ceramic glaze.

Table 4
Chemical composition of 90D glaze and of the different phases as analysed by EDX spectrometry

	SiO_2	Al_2O_3	Fe_2O_3	CaO	MgO	ZnO	K_2O
Average	60.26	8.63	2.45	12.32	2.82	9.07	4.46
Rounded crystals	30.25	8.19	31.57	5.84	2.93	18.83	2.39
Feather-like crystals	57.98	10.15	6.26	12.28	1.25	6.78	5.31

(Fig. 3a). This crystalline regions, which show irregular shape and size, are comprised by small rounded crystals whose average diameter is 0.75 μm (Fig. 3b). Table 4 collects the EDX analyses carried out on 90D glaze. As noted, rounded crystals show greater Fe_2O_3 and ZnO content when compared with the average composition, thus this crystalline phase could be identified as the zinc ferrite denominated franklinite ($ZnFe_2O_4$). EDX analysis

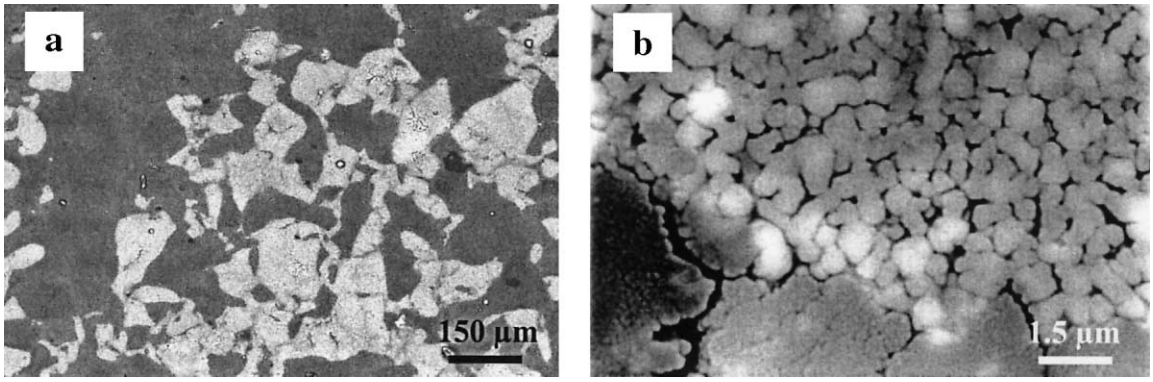

Fig. 4. SEM observations on the surface of 70D glass–ceramic glaze.

Table 5
Average chemical composition of 70D, 30D and 10 D glazes analysed by EDX spectrometry

	SiO_2	Al_2O_3	Fe_2O_3	CaO	MgO	ZnO	K_2O
70D	57.81	8.99	8.85	10.18	1.69	9.05	3.43
30D	52.35	11.65	18.85	7.67	1.94	3.15	4.39
10D	52.64	12.26	22.73	6.51	1.70	0.00	4.17

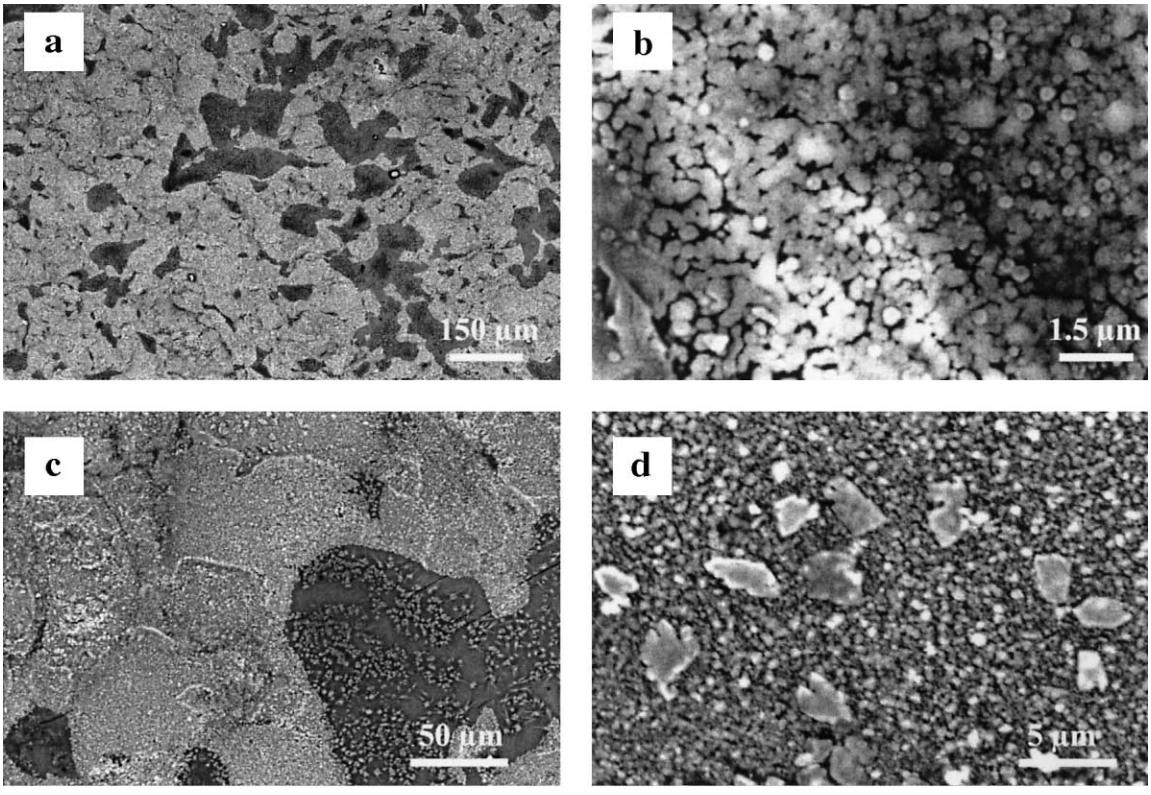

Fig. 5. SEM observations on the surface of 50D glass–ceramic glaze.

also shows a high SiO_2, Al_2O_3, CaO and K_2O contents; this is a consequence of the small size of franklinite crystals, which is down to the analytical resolution of the SEM/EDX system (1 μm). Because of its low percentage in the glaze (<2%), franklinite is not still detectable in he XRD pattern of 90D glaze (Fig. 1b). As well as 100D sample, diopside (parallelepiped crystals) and petedunnite (sail-like crystals) crystallise out of the parent glass (Fig. 3c). It can be observed that petedunnite is acting as nucleating agent of a new phase consisting of feather-like crystals. Those crystals, whose EDX analyses show a high Fe_2O_3 content, can be attributed to augite ($Ca(Mg, Fe)(SiO_3)_2$) or more likely to a half member of the pyroxene group, which undergoes a wide variety of ionic substitutions.[11,15] Augite shows a DRX pattern very similar to diopside and petedunnite giving rise to a overlapping of the three crystalline phases in the DRX diagram of 90D sample (Fig. 1b).

Fig. 4 shows the microstructure of 70D glaze, which is prepared with the addition of a 30% of granite frit. The X-ray spectra collected from this glaze (Fig. 1c) clearly shows a higher content of franklinite, also visible in the SEM observation (Fig. 4a), which show greater volume percentage of crystalline regions with high electron emission. The average diameter of franklinite crystals (Fig. 4b) is 0.60 μm, which is slightly lower than that showed in 90D glaze (0.75 μm). Table 5 shows the average EDX analysis carried out in this sample.

Fig. 5 shows the microstructure of the 50D sample. The addition of 50% of granite frit leads to a glass–ceramic glaze with franklinite as the main crystalline phase (Figs. 5a and 1d), with an average diameter of 0.45 μm (Fig. 5b). Parallelepiped and sail-like crystals of diopside and petedunnite are still present (Fig. 5c) and a new phase comprised of flake-like crystals, which are lying in franklinite regions, starts to crystallise (Fig. 5d). Table 6 shows the EDX analyses carried out on 50D

Table 6
Chemical composition of 5OD glaze and of the different phases as analysed by EDX spectrometry

	SiO_2	Al_2O	Fe_2O_3	CaO	MgO	ZnO	K_2O
Average	52.14	10.96	*14.56*	*9.51*	1.74	5.84	5.25
Flake-like crystals	47.70	11.14	25.34	7.21	2.26	1.79	4.57

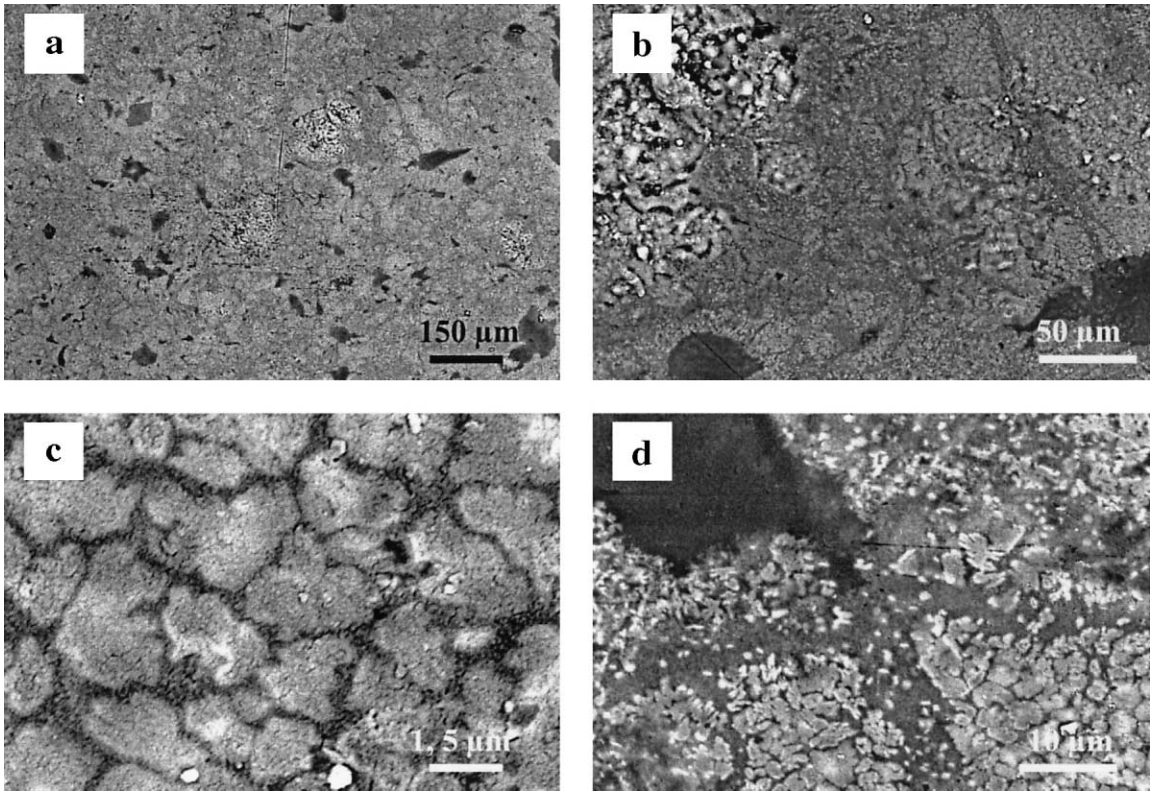

Fig. 6. SEM observations on the surface of 30D glass–ceramic glaze.

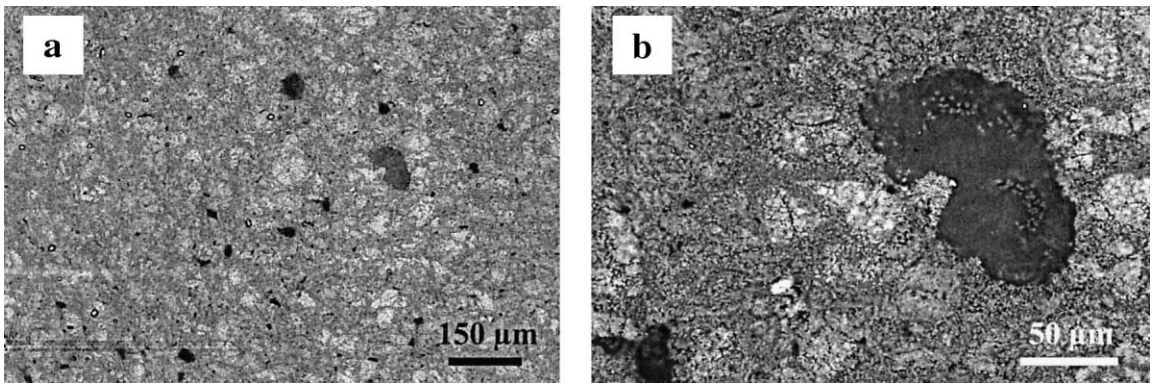

Fig. 7. SEM observations on the surface of 10D glass–ceramic glaze.

glaze. As noted, isolated flake-like crystals show greater Fe_2O_3 and lower ZnO content when compared with the average composition and with franklinite crystals (Table 4), respectively. Thus, this crystalline phase could be identified as hematite (Fe_2O_3), which is not yet detectable in he XRD pattern of 50D glaze (Fig. 1d). On the contrary, hematite is clearly identified in the XRD diffractogram of 30D glaze (Fig. 1e). Fig. 6 shows the SEM observations carried out on the surface of this glaze. It can be observed that the microstructure is very homogeneous (Fig. 6a) with almost all the surface filled by a continuous crystalline matrix with high white contrast. Hematite crystals, which appeared isolated in 5OD sample, are now assembled (Fig. 6b and c) whereas franklinite phase, which undergoes a morphological change, are present in the sample as dispersed blade-like crystal with an average size of 0.3×1.25 μm (Fig. 6d). The average EDX analysis of this sample is shown in Table 5.

Finally, Fig. 7 shows that the microstructure of 10D glaze, which is prepared with addition of 90% granite frit, is very similar to that observed in 30D glaze (Fig. 6). Although hematite is the main crystalline phase identified by XRD in this sample (Fig. 1f), SEM observations reveal that diopside and petedunnite are still present in this glass–ceramic glaze (Fig. 7b). The average EDX analysis of this sample is shown in Table 5.

Hence, the XRD and SEM/EDX results showed in the present study point out that iron content has a great influence on the oxidation state of iron ions in diopside glass–ceramic glazes. The authors are carried out additional investigations to determine if this iron effect is also showed by others glazes such as zircon-based glazes and high fusibility glazes.

4. Conclusion

The effect of iron content on crystallisation of a diopside glass–ceramic glaze has been stablished. XRD patterns and SEM observations on the surface of glass–ceramic glazes showed that the distribution of Fe^{3+} ions among several crystalline phases such as franklinite ($ZnFe_2O_4$) and hematite (Fe_2O_3) depends on the iron content in the frit mixture. Thus, an iron content lower than 9% (70D composition) leads to a glass-ceramic glaze with all Fe^{3+} ions crystallised as franklinite. An iron content close to 15% (50D mixture) gives rise to franklinite as main crystalline phase but Fe^{3+} ions start to crystallise as hematite. An iron content close to 19% (30D mixture) gives rise a change in the relative proportions of crystalline phases and hematite becomes the main crystalline phase crystallised out of the parent glass. Finally, an iron content greater than 22% (10D mixture) leads to a glass–ceramic glaze with all Fe^{3+} ions crystallised as hematite.

On the other hand, the size and morphology of franklinite is also influenced by the iron content in the frit mixture. So, franklinite crystallises as rounded crystals when $Fe_2O_3 < 15\%$ and as blade-like crystals for $Fe_2O_3 > 19\%$. As for crystal size, this decreases when iron content increase (from 0.75 μm for 90D mixture to 0.45 μm for 30D glaze).

As for diopside ($CaMg(SiO_3)_2$) and petedunnite ($CaZn(SiO_3)_2$)phases, their morphology and size is not depending of the iron content in the frit mixture. Diopside crystallises as parallelepiped crystals whereas petedunnite crystallise as sail-like crystals. Finally, SEM observation showed that petedunnite is acting as nucleating agent of feather-like crystals of augite ($Ca(Mg, Fe)(SiO_3)_2$).

Acknowledgements

The authors are greatly thankful to Fritta S.L. (Castellón, Spain).The experimental assistance of Mrs. P. Díaz (IETcc, Spain), Mr. C. Rivera (UC-LM, Spain) and Mr. A. Luna (UC-LM, Spain) is gratefully appreciated.

References

1. Rincón, J. M., Romero, M., Marco, J. and Caballer, V., Some aspects of crystallization microstructure on new glass–ceramic glazes. *Material Research Bulletin*, 1998, **33**(8), 1159–1164.
2. Romero, M. and Rincón, J. M., Preparation and properties of high iron oxide content glasses obtained from industrial wastes. *J. Eur. Ceram. Soc.*, 1998, **18**, 153–160.
3. Romero, M. and Rincón, J. M., Surface and bulk crystallization of glass–ceramic in the Na_2O–CaO–ZnO–Fe_2O_3–Al_2O_3–SiO_2 system derived from a goethite waste. *J. Am. Ceram. Soc.*, 1999, **82**(5), 113–117.
4. Barbieri, L., Manfredini, T., Queralt, I., Rincón, J. M. and Romero, M., Vitrification of fly ash from thermal power station. *Glass Technology*, 1997, **38**(5), 165–170.
5. Barbieri, L., Ferrari, A. M., Lancellotti, I., Leonelli, C., Rincón, J. M. and Romero, M., Crystallization of (Na_2O–MgO)–CaO–Al_2O_3–$5iO_2$ glassy systems formulated from waste products. *J. Am. Ceram. Soc.*, 2000, **83**(10), 2515–2520.
6. Rawlings, R. D., Production and properties of silceram glass–ceramic. In *Glass–ceramic Materials: Fundamentals and Applications*. Mucchi Editore, Modena, 1997.
7. Romero, M., Rawlings, R. D. and Rincón, J. M., Development of a new glass–ceramic by means of controlled vitrification and crystallisation of inorganic wastes from urban incineration. *J. Eur. Ceram. Soc.*, 1999, **19**, 2049–2058.
8. Rincón, J. M., Romero, M. and Boccaccini, A. R., Microstructural characterisation of a glass and a glass–ceramic obtained from municipal incinerator fly ash. *J. Mater. Sci.*, 1999, **34**, 4413–4423.
9. Romero, M., Rawlings, R. D. and Rincón, J. M., Nucleation and crystal growth in glasses from inorganic waste from urban incineration. *J. Non-Cryst. Solids*, 2000, **271**(1–2), 106–118.
10. Boccaccini, A. R., Romero, M. and Rincón, J. M., Sintered glass–ceramics from municipal incinerator fly ash. *Glass Technology*, 2000, **41**(6), 99–105.
11. Romero, M., Rincón, J. M., Rawlings, R. D. and Boccaccini, A. R., Use of vitrified urban incinerator waste as raw material for production of sintered glass–ceramics. *Materials Research Bulletin*, 2001, **36**(2).
12. Zubekhin, A. P., Zhabrev, V. A. and Kondyurin, A. M., Glass formation and crystallization in the SiO_2–CaO–MgO–Fe_2O_3–MnO_2–K_2O–Na_2O for synthesizing heat resistant coatings. *Steklo i Keramica*, 1993, **5**, 26–28.
13. Brawer, S. A. and White, W. B., Structure and crystallization behaviour of Li_2O–Fe_2O_3–SiO_2 glasses. *J. Mater. Sci.*, 1978, **13**, 1907.
14. Salman, S. M. and Salama, S. N., Pyroxene solid solution crystallized from CaO–MgO–(Li_2O, Fe_2O_3)–SiO_2 glasses. *Ceramics Int*, 1986, **12**, 221–228.
15. Deer, W. A., Howie, R. A. and Zussman, J., *Rock Forming Minerals. Vol. 2*. Longman, London, 1963.